Available online at www.sciencedirect.com
ScienceDirect
JOURNAL OF RARE EARTHS
www.re-journal.com/en/
JOURNAL OF RARE EARTHS, Vol. 29, No. 12, Dec. 2011, P. 1178

Development of novel rare earth doped fluoride and oxide scintillators for two-dimensional imaging

A. Yoshikawa[1,2], T. Yanagida[2], Y. Yokota[1], K. Kamada[1], N. Kawaguchi[1,3], K. Fukuda[1,3], A. Yamazaki[4], K. Watanabe[4], A. Uritani[4], T. Iguchi[4], G. Boulon[1,5], M. Nikl[6]

(1. Institute for Materials Research, Tohoku University, 2-1-1 Katahira, Aoba-ku, Sendai 980-8577, Japan; 2. New Industry Creation Hatchery Center, Tohoku University, 6-6-10 Aoba, Aramaki, Aoba-ku, Sendai, Miyagi 980-8579, Japan; 3. R&D Center, Tokuyama Corporation, Shibuya 3-Chome, Shibuya-ku, Tokyo 150-8383, Japan; 4. Nagoya University, Furo-cho, Chikusa-ku, Nagoya, 464-8601, Japan; 5. Physical Chemistry of Luminescent Materials (LPCML), University of Lyon, UCBLyon1, UMR 5620 CNRS, 69622 Villeurbanne, France; 6. Institute of Physics AS CR, Cukrovarnicka 10, 162 53 Prague, Czech Republic)

Received 26 August 2011; revised 5 September 2011

Abstract: Two topics were focused. The first one was about the gamma-ray scintillator, Pr^{3+}:$Lu_3Al_5O_{12}$ (LuAG). The second one was about neutron scintillator, Ce^{3+}:^{6}LiCaAlF$_6$ and Eu^{2+}:^{6}LiCaAlF$_6$ (^{6}LiCAF). Those scintillators have been developed very recently for modern imaging applications in the medical and homeland security fields. In both cases, the rare earth ions are playing the crucial role as emission centers. Pr^{3+} in LuAG provided fast 5d→4f transition providing noticeably shorter decay time than that of Ce^{3+}. Among several candidate hosts, LuAG showed the best performance. Bulk crystal growth, basic scintillation properties, two-dimensional gamma-ray imaging and positron emission mammography (PEM) application were demonstrated. Due to the international situation, the homeland security was compromized by illicit traffic of explosives, drugs, nuclear materials, etc. and the ways to its improvement became an important R&D topic. For this purpose the Ce and Eu doped LiCAF appeared competitive candidates. Especially, when substitution of ^{3}He neutron detectors was considered, the discrimination ability of gamma-ray from alpha-ray was important. Bulk crystal growth, basic scintillation properties and two-dimensional neutron imaging were demonstrated.

Keywords: Scintillator; gamma-ray detection; neutron detection; oxide; fluoride; Ce, Eu; rare earth

Single crystal scintillator materials are widely used for detection of high-energy photons and particles. There is continuous demand for new scintillator materials with higher performance because of increasing number of medical, industrial, security and other applications[1].

In the case of modern scintillators, the high light output, good energy resolution, high effective atomic number, fast scintillation response, chemical stability and capability of bulk crystal growth are very important parameters. Especially, medical imaging techniques which are based on the coincidence measurements, requires very fast scintillation decay. Generally, the decay rate Γ of an excited state is given by following equation (Eq. 1)[2,3]:

$$\Gamma = \frac{1}{\tau} \propto \frac{n}{\lambda_{em}^3}\left(\frac{n^2+2}{3}\right)^2 \sum_f |< f|\mu|i >|^2 \quad (1)$$

where, Γ is transition probability, τ is decay time, n is refractive index, λ_{em} is emission wavelength, f and i are the ground and excited state wave functions, respectively, and μ is dipole operator.

As far as we are studying the Ce^{3+} doped oxides the emission wavelength is typically from 350 to 550 nm and the decay time determined by the 5d→4f transition of Ce^{3+} is typically within 20–60 ns. Only rare earth halide host provided the faster Ce^{3+} 5d→4f emission with decay time less than 20 ns[3–5]. However, their extreme hygroscopicity strongly limits their application potential. Therefore, the emission due to Pr^{3+} 5d-4f transition can be the promising candidate to obtain typically 2–3 times faster scintillation response.

Neutron detection is an essential aspect of interdiction of radiological threats for national security purposes, since plutonium, a material used for nuclear weapons, is a significant source of fission neutrons. The current demand for ^{3}He in commonly deployed neutron detectors and other systems has created an imminent shortage of ^{3}He due to its limited natural resources. Therefore, an alternative technological solution for neutron detection is required in the very near future[6]. Neutron detector is used not only for security purposes but also in scientific research, e.g. neutron diffraction to investigate the positioning of light elements in the crystal structure. This is also nowadays topic, as the Li based fuel cell becomes highly important. So far, five technologies, boron trifluoride (BF_3) filled proportional detectors[7,8], boron-lined proportional detectors, scintillating glass fiber detectors, scintillator coated wavelength-shifting fiber detectors, and ^{6}Li based or ^{10}B based bulk neutron scintillators, are proposed as

Foundation item: Project supported by Japan Science and Technology Agency, Regional Research and Development Resources Utilization Program, Ministry of Education, Culture, Sports, Science and Technology of Japanese government, Grant-in-Aid for Young Scientists (A), the joint project between JSPS and ASCR (19686001 (AY)), Czech GAAV Project (M100100910) and the Funding Program for Next Generation World-Leading Researchers, Japan Society for Promotion of Science

Corresponding author: A. Yoshikawa (**E-mail:** yoshikawa@imr.tohoku.ac.jp; **Tel.:** +81-22-215-2217)

DOI: 10.1016/S1002-0721(10)60621-7

the alternative candidates. In order to realize the simple system for neutron detection, BF_3 and bulk neutron scintillators are the most promising candidates. As BF_3 gas is toxic[9], it can not be the alternatives for ^{3}He. Therefore, highly efficient neutron scintillator as well as the bulk crystal growth technologies have to be developed.

Based on the above mentioned background and our recent results, we review two topics: (i) Pr^{3+}:$Lu_3Al_5O_{12}$(LuAG) for gamma-ray scintillator[10–13]; (ii) Ce^{3+}:^{6}LiCaAlF$_6$ (Ce:^{6}LiCAF)[14,15] and Eu^{2+}:^{6}LiCaAlF$_6$ (Eu:^{6}LiCAF)[16] for neutron scintillator. In all the cases, rare earth ions are playing an important role as the emission centers in the above mentioned host structures.

1 Experimental

1.1 Synthesis

1.1.1 Crystal growth of Pr:LuAG Starting materials were Pr_6O_{11}, Lu_2O_3 and α-Al_2O_3 powders with purity of 99.99%. Iridium crucible was used and heated by radio frequency (RF) induction up to melting temperature (around 2000 °C) under Ar atmosphere. Growth orientation was controlled by the [111]-oriented undoped LuAG single crystalline seed. Crystal rotation rate was ~10 r/min, and the growth pulling rate was 1.0 mm/h.

1.1.2 Crystal growth of Ce doped and Eu doped LiCAF Starting materials were LiF, CaF_2, AlF_3, EuF_3 powders with a purity of 99.99%. Graphite crucible was used and heated by radio frequency (RF) induction up to melting temperature (around 900 °C) in Ar(95%)+CF_4(5%) atmosphere[17]. Growth orientation was controlled by the [001]-oriented undoped LiCAF single crystalline seed. Crystal rotation rate was ~10 r/min, and the growth pulling rate was 0.5–1.5 mm/h.

1.2 Characterization and performance test

1.2.1 Pr:LuAG After cutting and polishing the as grown crystal, optical properties were studied. Optical transmission spectra were measured using a JASCO V550 spectrophotometer. Luminescence measurements were carried out using spectrofluorometer FLS920 (Edinburgh Instruments) equipped with the hydrogen steady-state, nanosecond and Xe microsecond pulsed flashlamps (IBH Scotland). Spectral range of both equipments is 200 to 900 nm.

For the scintillation properties measurement, the crystals were covered with several layers of Teflon tape and optically coupled to the light entrance window of photo-multiplier tube (PMT) R7600 (Hamatsu) with an optical grease. The high voltage was supplied by ORTEC 556, and signals were red out from the anode of PMT. Then, the signals passed a shaping amplifier ORTEC 570 with 0.5 μs shaping time, converted to digital signals by a multi channel analyzer Pocket MCA 8000A provided by Amptek Co. and recorded in a computer. Decay time was also evaluated using an oscilloscope, Tektronix TDS3034B.

As for the 2 dimensional imaging test, Pr:LuAG pixel array (1 pixel: 2 mm square, 20×20 pixels) were prepared using $BaSO_4$ as reflector. $BaSO_4$ powder was mixed with an adhesive and ethanol. Acrylic-type adhesive which has high transparency around 310 nm was selected. The 0.1 mm thick layer of this mixture was deposited onto each crystal. The pixelated scintillator array was optically coupled with H8500 photomultiplier to study its performance as a gamma camera. The optical coupling was enabled by silicon grease (OKEN 6262A). After coupling, the detector array was irradiated by the 662 keV gamma-ray (^{137}Cs) from the top side.

All the experiments were carried out at room temperature.

1.2.2 Ce:LiCAF and Eu:LiCAF Transmission spectra were obtained with the spectrometer JASCO, V-530. Luminescence measurements were performed with the spectrofluorometer FLS920 (Edinburgh Instruments) equipped with the hydrogen steady-state lamp. ^{241}Am was used as an α-ray source. In order to see the response after thermal neutron excitation, ^{252}Cf neutron radiation was used to excite the sample, Pb plate was inserted to remove gamma-ray. Photoelectron yield was compared with a standard reference ^{6}Li enriched solid state neutron scintillator, such as Li-glass scintillator (GS20, Saint Gobain). A photomultiplier tube (PMT, Hamamatsu, H7416) was used as a photodetector. All measurements were made at room temperature.

Neutron imaging using Ce doped $LiCaAlF_6$ scintillator and PSPMT which had 64 channel multi-anode were demonstrated. Obtained crystal was cut to the circular plate shape with the size of Φ55 mm and 2 mm thickness and optically coupled to PSPMT by silicone grease (OKEN 6262A). The sealed ^{252}Cf source (<1 MBq) was used with a thickness of 43 mm polyethylene for neutron thermalization. Alphabet-shape Cd pieces with a thickness of 4 mm were used as a mask of thermal neutron. Signal at each anode was fed into preamplifier, followed by the shaping amplifier with 5 μs integration and the personal computer.

2 Results and discussion

2.1 Pr:LuAG

Growth conditions such as pulling rate, rotation rate, and insulator design in the furnace were optimized for obtaining crack free 2-inch-diameter Pr:LuAG crystals with uniform light output and decay time in whole crystal. 2-inch-diameter 2.5%Pr:LuAG single crystals with a length of 110 mm was grown with a nominal composition of $(Pr_{0.075}Lu_{2.925})Al_5O_{12}$ (Fig. 1). The solidification yield of Pr:LuAG for raw materi-

Fig. 1 2-inch-diameter bulk Pr:LuAG single crystal grown by the Cz method

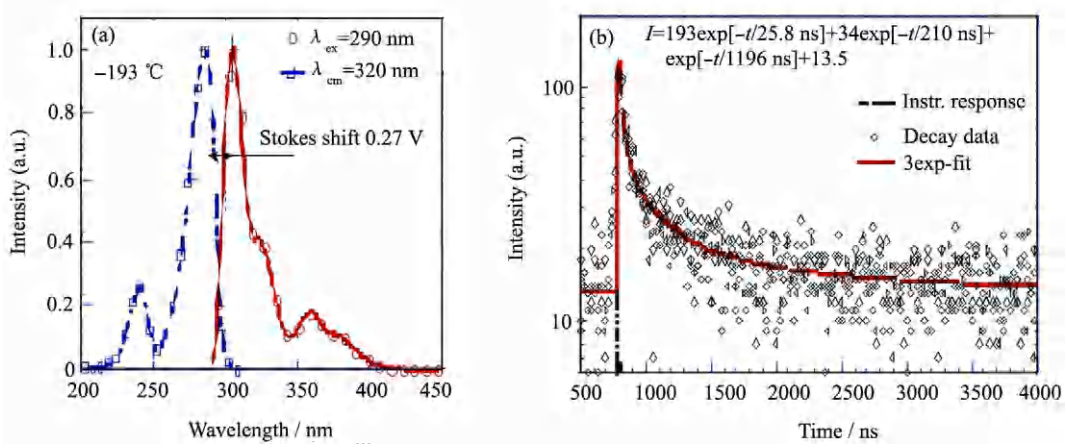

Fig. 2 Excitation and emission spectra of Pr:LuAG (a) and scintillation decay of Pr:LuAG (b)

als was about 40% of melt of raw material in the crucible.

Excitation and emission spectra of Pr:LuAG is shown in Fig. 2(a). Pr^{3+} 5d→4f transitions are dominating both spectra[11] and the stokes shift is found as 0.27 eV. Scintillation decay of Pr:LuAG dominated by 26 ns decay time is shown in (b), slower component with 210 and 1200 ns decay time are clearly visible as well.

The ^{137}Cs gamma-ray image using a test detector consisting of 20×20 pixelated array is shown in Fig. 3.

1.3.2 Ce:LiCAF and Eu:LiCAF Growth conditions such as pulling rate, rotation rate, and insulator design in the furnace were optimized for obtaining crack free 2-inch-diameter Ce and Eu doped LiCAF crystals with Colquiriite-type structure. As shown in Fig. 4, 2-inch-diameter 2.0%Ce:LiCAF and 2%Eu:LiCAF single crystals (nominal composition) with a length of 100 mm were grown by the Cz method. Both crystal were transparent and have no visible inclusions and cracks.

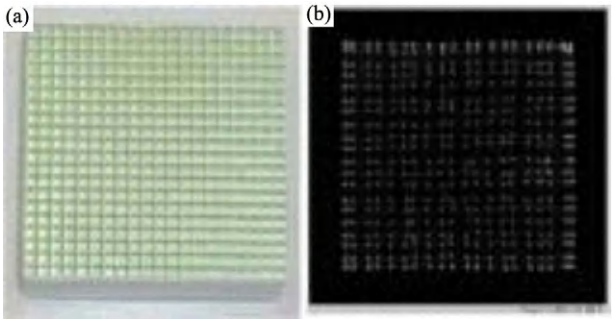

Fig. 3 20×20 Pr:LuAG pixelated array (a) and 2-dimensional image under ^{137}Cs irradiation (b)

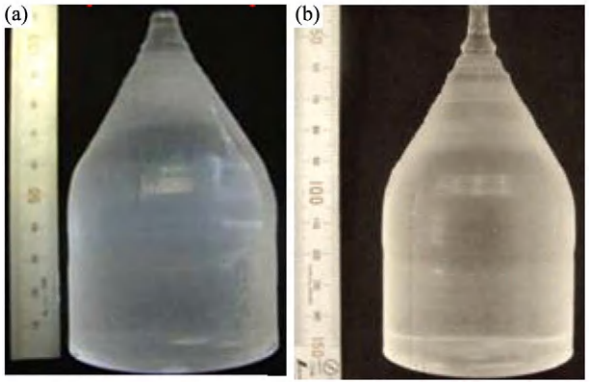

Fig. 4 2-inch-diameter bulk Ce:LiCAF (a) and Eu:LiCAF single crystal (b) grown by the Cz method

Transmission and emission spectra of Ce:LiCAF and Eu:LiCAF are shown in Fig. 5. Ce^{3+} and Eu^{2+} 5d-4f transitions are clearly observed. The observed characteristics are consistent with earlier reports at these materials studied under UV and gamma excitations[17,18]. While the decay time of the Ce^{3+} center in LiCAF host is of about 20–35 ns[17], and that of Eu^{2+} is longer of about 1–1.2 μs[16,18].

α/β ratio of Ce:LiCAF and Eu:LiCAF crystals are shown in Fig. 6. It was observed that the α/β ratios for Ce:LiCAF or Eu:LiCAF are different. This was found by the Soltan Institute for Nuclear Studies[19].

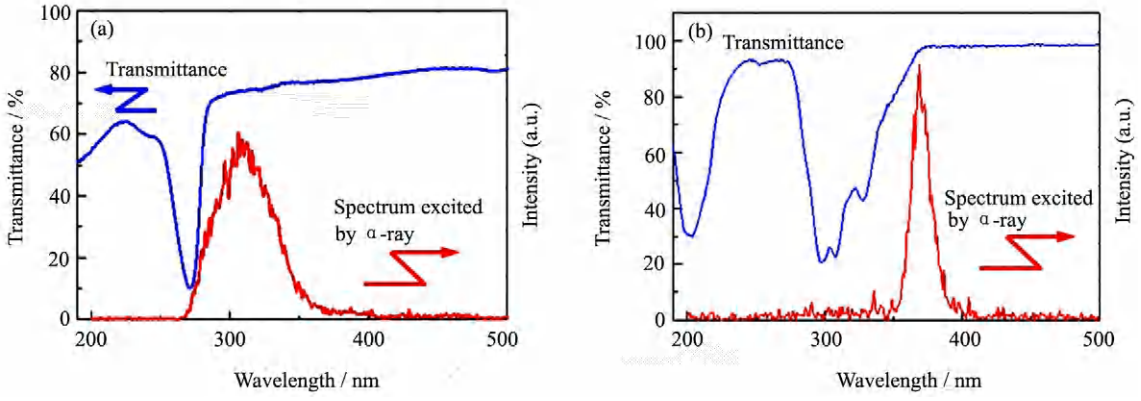

Fig. 5 Transmittance and emission spectra of Ce:LiCAF (a) and Eu:LiCAF (b)

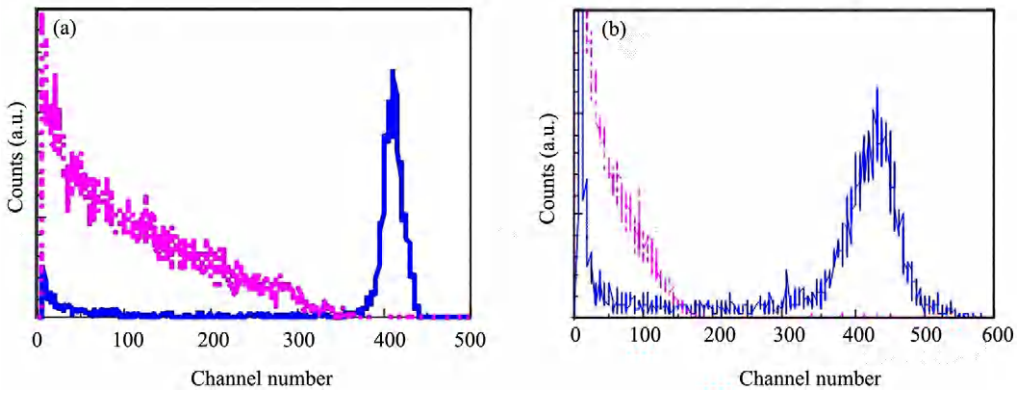

Fig. 6 α/β ratio of Ce:LiCAF (a) and Eu:LiCAF crystals (b)

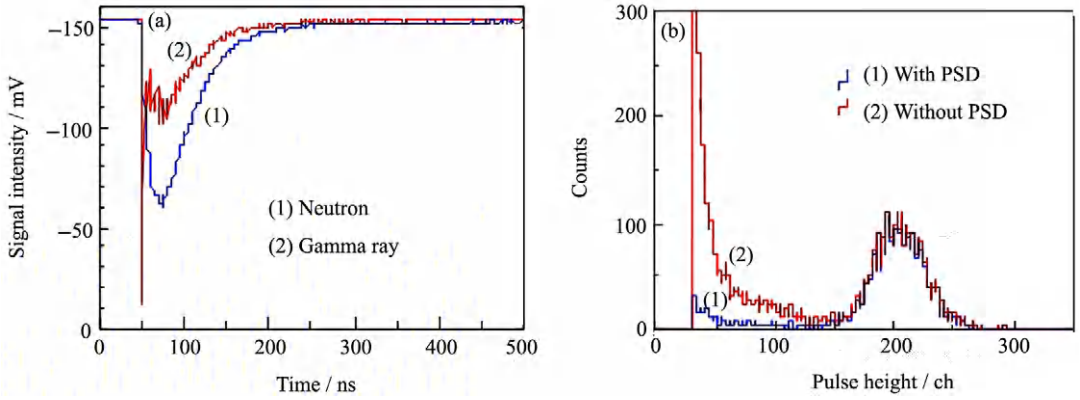

Fig. 7 Deferent pulse shapes for neutron and γ-ray irradiation in Ce:LiCAF (a) and pulse height spectra of Ce:LiCAF with and without PSD (b)

Nagoya University group found that Ce:LiCAF has deferent pulse shapes for neutron and γ-ray irradiation, and pulse shape discrimination were carried out as shown in Fig. 7[20,21]. This featurte is of great advantage to better discriminate the inevitable gamma background in neutron fluxes[21].

As shown in Fig. 8, two dimensional neutron imaging was obtained using LiCAF plate with PS-PMT. The parallel beam of thermal neutron source at JRR-3, MUSASI (JAEA) was used. The neutron flux was around 8×10^5 counts/s.

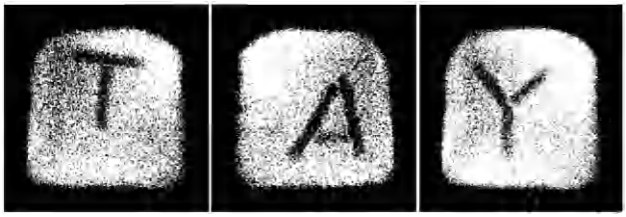

Fig. 8 Two dimensional neutron imaging using the Cd mask[16]

3 Conclusions

Crystal growth, absorption, photo- and radioluminescence spectra, as well as the performance test of Pr^{3+}:LuAG gamma-ray scintillator and Ce^{3+}:^{6}LiCAF and Eu^{2+}:^{6}LiCAF neutron scintillator were surveyed. Due to the mastered growth technology of big enough single crystals and competitive combination of scintillation parameters, these materials have great practical prospectives. Pr^{3+} in LuAG provided fast 5d→4f transition providing noticeably shorter decay time with respect to that of Ce^{3+}. As LuAG showed the best performance, after the development of technology on bulk crystal growth, basic scintillation properties and two-dimensional gamma-ray imaging, positron emission mammography (PEM) was conducted on Pr:LuAG. As a candidate for alternatives of ^{3}He neutron detectors, Ce and Eu doped LiCAF appeared competitive candidates. For this purpose, the discrimination ability of gamma-ray from alpha-ray is important. Therefore, pulse shape discrimination was investigated and succeeded. Bulk crystal growth, basic scintillation properties and two-dimensional neutron imaging were demonstrated, as well.

References:

[1] Weber M J. Inorganic scintillators: today and tomorrow. *J. Lumin*., 2002, **100**: 35.

[2] Henderson B, Imbush G F. Optical Spectroscopy of Inorganic Solids. Oxford: Clarendon Press, 1989.

[3] Dorenbos P. Light output and energy resolution of Ce^{3+}-doped scintillators. *Nucl. Instr. Methods Phys. Res. Sect. A,* 2002, **486**: 208.

[4] van Loef E V D, Dorenbos P, van Eijk C W E, Krämer K, Güdel H U. High-energy-resolution scintillator: Ce^{3+} activated $LaCl_3$. *Appl. Phys. Lett*., 2000, **77**: 1467.

[5] van Loef E V D, Dorenbos P, van Eijk C W E, Krämer K, Güdel H U. High-energy-resolution scintillator: Ce^{3+} activated $LaBr_3$. *Appl. Phys. Lett*., 2001, **79**: 1573.

[6] Kouzes R T, Ely J H, Erikson L E, Kernan W J, Lintereur A T, Siciliano E R, Stephens D L, Stromswold D C, VanGinhoven R M, Woodring M L. Neutron detection alternatives to ^{3}He for national security applications. *Nucl. Instrum. Methods Phys.*

Res. Sect. A, 2010, **A623**: 1035.

[7] Hanson A O, McKibben J L. A neutron detector having uniform sensitivity from 10 KeV to 3 MeV. *Physical Review*, 1947, **72**: 673.

[8] Bolewski Jr. A, Ciechanowski M, Dydejczyk A, Kreft A. On the optimization of the isotopic neutron source method for measuring the thermal neutron absorption cross section: Advantages and disadvantages of BF_3 and ^3He counters. *Applied Radiation and Isotopes*, 2008, **66**: 457.

[9] CAS 7637-07-2 Chemical Profile for Boron Trifluoride: http://www.chemindustry.com/chemicals/651983.html

[10] Yoshikawa A, Kamada K, Ogino H, Aoki K, Fukuda T. Pr containing single crystal for scintillator, process for producing the same, radiation detector and inspection apparatus. PCT/JP2005/020386

[11] Nikl M, Ogino H, Krasnikov A, Beitlerova A, Yoshikawa A, Fukuda T. Photo- and radioluminescence of Pr-doped $Lu_3Al_5O_{12}$ single crystal. *Phys. Stat. Sol. (a)*, 2005, **202**: R4.

[12] Yoshikawa A, Yanagida T, Kamada K, Yokota Y, Pejchal J, Yamaji A, Usuki Y, Yamamoto S, Miyake M, Kumagai K, Sasaki K, dos Santos T R, Baba M, Ito M, Takeda M, Ohuchi N, Nikl M. Positron emission mammography using Pr:LuAG scintillator-fusion of optical material study and systems engineering, *Opt. Mater.*, 2010, **32**: 1294.

[13] Drozdowski W, Dorenbos P, de Haas J T M, Drozdowska R, Owens A, Kamada K, Tsutsumi K, Usuki Y, Yanagida T, Yoshikawa A. Scintillation properties of praseodymium activated $Lu_3Al_5O_{12}$ single crystals. *IEEE Trans. Nucl. Sci.*, 2009, **56**: 3796.

[14] Yoshikawa A, Yanagida T, Yokota Y, Kawaguchi N, Ishizu S, Fukuda K, Suyama T, Kim K J, Nikl M, Miyake M, Baba M. Single crystal growth, optical properties and neutron response of Ce^{3+} doped $LiCaAlF_6$. *IEEE. Nucl. Trans. Sci.*, 2009, **56**: 3796.

[15] Yamazaki A, Watanabe K, Uritani A, Iguchi T, Kawaguchi N, Yanagida T, Fujimoto Y, Yokota Y, Kamada K, Fukuda K, Suyama T, Yoshikawa A. Neutron/gamma discrimination based on pulse shape discrimination in a Ce:$LiCaAlF_6$ scintillator. *Nucl. Instrum. Methods Phys. Res. Sect. A*, 2011, **652**: 435.

[16] Yanagida T, Kawaguchi N, Fujimoto Y, Fukuda K, Yokota Y, Yamazaki A, Watanabe K, Pejchal J, Uritani A, Iguchi T, Yoshikawa A. Basic study of Europium doped $LiCaAlF_6$ scintillator and its capability for thermal neutron imaging application. *Opt. Mater*., 2011, **33**: 1243.

[17] Nikl M, Solovieva N, Mihokova E, Dusek M, Vedda A, Martini M, Shimamura K, Fukuda T. Scintillation decay of $LiCaAlF_6:Ce^{3+}$ single crystals. *Phys. Stat. Sol. (a)*, 2001, **187**: R1.

[18] Shiran N V, Gektin A V, Neicheva S V, Kornienko V A, Shimamura K, Ishinose N. Optical and scintillation properties of $LiCaAlF_6$:Eu crystal . *J. Lumin*., 2003, **102-103**: 815.

[19] Iwanowska J, Swiderski L, Moszynski M, Szczesniak T, Sibczynski P, Galunov N Z, Karavaeva N L. Neutron/gamma discrimination properties of composite scintillation detectors. *Journal of Instrumentation*, 2011, **6**: 07007.

[20] Yamazaki A, Watanabe K, Uritani A, Iguchi T, Kawaguchi N, Yanagida T, Fujimoto Y, Yokota Y, Kamada K, Fukuda K, Suyama T, Yoshikawa A. Neutron-gamma discrimination based on pulse shape discrimination in a Ce:$LiCaAlF_6$ scintillator. *Nucl. Instrum. Methods Phys. Res. Sect. A,* 2011, **652**: 435.

[21] Carel W E van Eijk. Inorganic scintillators for thermal neutron detection. *Radiation Measurements*, 2004, **38**: 337.